Application of a Photoacoustic Sensor for Colon Cancer Imaging: A Case Report[I]

Ashkan Ghanbarzadeh-Daghyean[1,*], Francis Kalloor Joseph[1], Cyrille Mooij[2], Stefan van der Stel[2], Theo Ruers[2]
[1]*Biomedical Phototonic Imaging (BMPI), University of Twente, Enschede, The Netherlands*
[2]*National Cancer Institute (NKI), Amsterdam, The Netherlands*
[*]*a.dagheyan@utwente.nl*

***Abstract*—The incidence of colorectal cancer is on the rise on a global scale. Besides research into novel treatment schemes, accurate monitoring techniques are necessary to help in the process, especially for the post-treatment period. Recently, photoacoustic (PA) imaging has been investigated as a tool for detecting and monitoring colon cancer, with a potential of distinguishing various tissue types. In this initial study, we report using an LED-based PA sensor on a colon cancer specimen, *ex-vivo*. Our initial data with an LED of a wavelength equal to 850 nm shows that the PA signal is weaker in the malignant region when compared to healthy colon tissue or fat, while stronger than the signal in water (noise level). These results pave the way for larger studies, including data from more patients and various types of tumors.**

***Index Terms*—ultrasound, photoacoustics, colon cancer, cancer detection**

I. Introduction

In 2020, 1.9 million new cases of colorectal cancer (CRC) and 930,000 deaths due to this disease were reported. These figures are projected to increase to 3.2 million new cases and 1.6 million deaths by 2040 [1]. Unhealthy lifestyle is the main cause of the onset of CRC, with the most important risk factors being a diet low in fiber and high in processed meat, low physical activity, and high consumption of tobacco and alcohol [2]. Standard treatment options include chemotherapy, radiation therapy, adjuvant therapy, endoscopic treatment and surgery [3].

Early detection and monitoring of cancer is an essential part of a successful treatment. In addition, accurate and timely monitoring of CRC could help prevent cancer recurrence. However, the current methods of post-treatment surveillance of CRC patients, including colonoscopy and CT imaging, have their own drawbacks, and recent reviews have challenged their cost-effectiveness [4]. For example, there are risks associated with the radiation from CT, especially if the patient is monitored frequently. Meanwhile, new methods are under investigation for surveillance of CRC, with the goal of compensating some of the mentioned shortcomings. Recently, a particular attention has been drawn to photoacoustic imaging (PAI) of colon cancer [5].

In PAI, the tissue is irradiated with periodic laser pulses, which generate ultrasound (US) waves because of the tissue expansion, which is due to instantaneous temperature rise in the tissue. These waves are then detected by an ultrasound receiver (or transducer), which are processed into a photoacoustic (PA) image [6]. The PA effect can be described using the following equation in space and time:

$$(\nabla^2 - \frac{1}{c^2}\frac{\partial^2}{\partial t^2})p(\mathbf{r},t) = -\frac{\beta}{\kappa c^2}\frac{\partial^2 T(\mathbf{r},t)}{\partial t^2}, \quad (1)$$

where the definition of the parameters are as follows:
c: speed of sound (m/s),
$p(\mathbf{r},t)$: change in acoustic pressure (Pa) at location $\mathbf{r}$ and time t,
β: the thermal coefficient of volume expansion (K^{-1}),
κ: the isothermal compressibility (Pa^{-1}), and
$p(\mathbf{r},t)$: change in temperature (due to laser pulses) at location $\mathbf{r}$ and time t.

In recent years, the use of PA microscopy has been reported for colorectal cancer detection and monitoring, with innovations such as the development of a PA endoscope and AI-based automatic classification based on features in US and PA

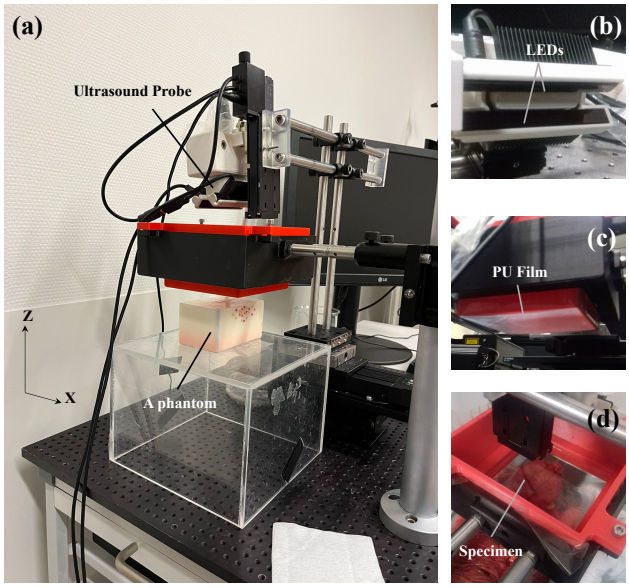

Fig. 1. The *ex-vivo* experimental setup: (a) The US probe and LEDs placed above the water container (red-black), (b) the 850-nm LED placed on two sides of the US probe, (c) the PU film installed in a stretched manner at the window of the water container, (d) the water container and the PU film pressed against the specimen.

I. This work has been funded by University of Twente.

2023 IEEE SENSORS | 979-8-3503-0387-2/23/$31.00 ©2023 IEEE | DOI: 10.1109/SENSORS56945.2023.10325225

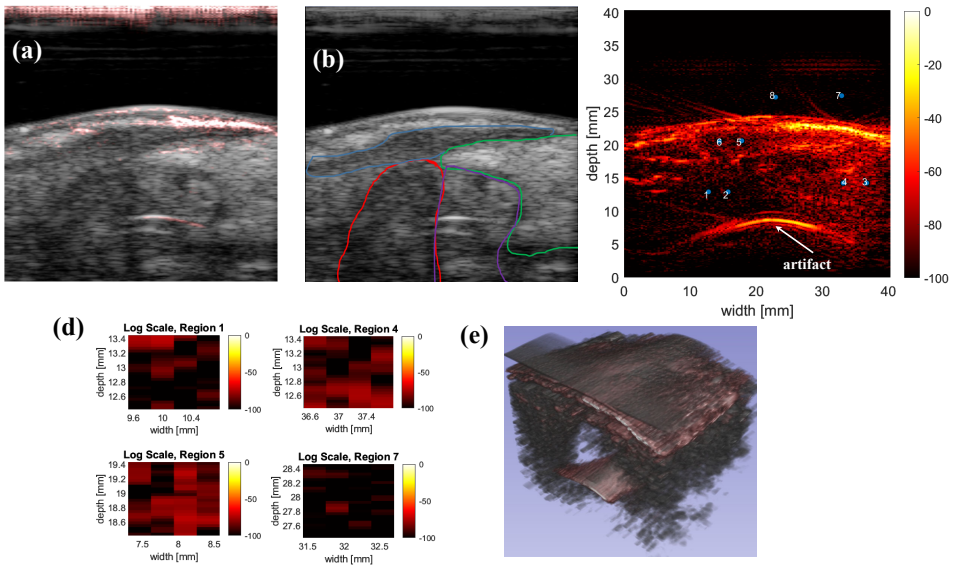

Fig. 2. (a)-(d) Post-processing of an image that contains tissues of interest: (a) PA image laid over the US image, (b) US image annotated by physicians (blue: healthy colon tissue, red: tumor, purple: unknown, green: fat), (c) high-quality PA image with selected points (1,2 in tumor; 3,4 in fat; 5,6 in healthy colon tissue, 7,6 in water (noise level)), (d) example of selected regions for averaging pixel values, (e) a 3D rendering of the 20-mm sweep (for visualization)

images [7]. Here, for the first time, we report PAI of an *ex-vivo* colon cancer specimen using the LED-based commercial PA system *AcousticX* (Cyberdyne, Japan), which generates co-registered US and PA images [8]. In *AcousticX*, instead of laser beams, LEDs with various wavelengths are used to generate the PA effect. As the first case study, we present some of the observations made from images obtained from the specimen.

II. Methods

A. Ex-vivo Specimen

The fresh colon specimen was obtained from a surgery on a cancer patient receiving treatment at the National Cancer Institute (NKI) of the Netherlands. The use of the specimen for this study was approved by the NKI and written consent was obtained from the patient. The specimen was cleaned by the pathology department and transferred to the measurement room where *AcousticX* was placed.

B. Experimental Setup

Two 850-nm LEDs were selected for this study. A holder was designed to keep the LEDs on the two sides of a 7-MHz ultrasound probe (Fig. 1-(a) and -(b)). The probe was also installed on a holder, where it could be moved via a motorized stage, up and down (along the *Z* axis) and left and right (the *Y* axis). The Z-axis motor was operated manually and the X-axis motor was connected to *AcousticX* and was operated via the system's GUI.

To prevent the specimen from contamination and to create impedance matching between the US probe and the tissue, a container was designed with an ultrasound window underneath it. A sterile polyurethane (PU, Protection Cover Ultrasound B.V., The Netherlands) film was installed, and kept stretched, on the ultrasound window (Fig. 1-(c)). A small amount of NaCl serum was poured over the specimen to fill the parts that contained air with liquid.

After the container and the film were pressed against the sample (Fig. 1-(d)), an adequate amount of water was poured in the container to cover the head of the ultrasound probe and the LEDs, and to act as a matching liquid between the probe and the tissue. Bubbles between the film and the tissue were removed using a finger, through the water, without touching the specimen. Finally, the probe was brought down into the water and within about 5 mm of the the PU film to acquire data.

C. Data Acquisition and Post-processing

Using the *AcousticX* GUI, two datasets were collected: (1) PA and US data via a 20-mm linear sweep, for 3D visualization of the tissue, and (2) PA and US date via a stop and scan (SnS) scheme with five acquisitions along a 20 mm section of the tissue. The RF data of all the measurements and screenshots of all the measurements were recorded. The US images of two frames that contained all types of tissues of interest (one shown in Fig. 2-(a)), generated by *AcousticX*, were used by physicians at the NKI to annotate the image and localize the malignant (M), fatty (F), and healthy-colon (H) tissue (Fig. 2-(b)). PA data was separately processed off-line for high-quality images, by averaging over 10 frames.

To compare the PA signal values in different regions of the PA images, two points were selected in each annotated region and the values were averaged in a square over the image pixels within 2 mm around the point (Fig. 2-(c) and -(d)). The region size was selected to be the same for all sample points. For mean and error analysis, both points in the same tissue region were considered (stacked in one vector). Averaging over the whole annotated regions was avoided due to presence of

artifacts in some parts of the PA image, because it would affect the average value considerably.

Figure 2-(e) shows a 3D reconstruction of the 83 frames acquired during the 20-mm sweep, including the PA (red) and US (gray) data. Such images help physicians further with tissue annotation and detecting possible PA artifacts.

III. Results and Discussion

Figure 3 shows the results of the analysis for the selected points and regions in the image shown in Fig. 2 and another image that similarly contained all the tissues of interest. The mean values alongside the standard errors are presented for each region (taking into account both points in each region). The mean of noise level is lower than the mean values of all regions. Based on this initial data, the PA signal is weaker in the tumor region than in the healthy and fatty tissue. However, the same cannot be said about fat and healthy colon tissue as they exhibit opposite comparisons in Fig. 3-(a) and -(b).

At the current stage of the project, the amount of data is limited in this study to draw definite conclusions. However, several observations can be made:

1) The use of the LED-based PA probe is viable for ex-vivo colon studies.
2) The design of the system, including the water container and its US window and, motorized motion, enables semi-automated data collection in sweep and SnS modes.
3) Based on this initial data, the malignant area seems to generate PA signals weaker than healthy tissue, whether from fat or colon.

This initial data and analysis paves the way for further studies, including specimens from more patients. Furthermore, more robust analysis methods can be devised. For example, given that with the present approach, the PA signal values are relative, having a reference object in the imaging scene could enable a more quantitative way of comparing results, especially across patients. Also, the effect of depth on the strength of the signal due to absorption needs to be investigated.

IV. Conclusions

This study focused on using an LED-based photoacoustic sensor to acquire data from a colon cancer specimen, *ex-vivo*, for the first time. The imaging system contains a motorized stage and a water container and a polyurethane-film ultrasound window for contact with the tissue. The early results from the analysis of the PA signal value in different regions of the tissue (malignant, fat, and healthy tissue of colon) show that the malignant tissue has lower mean PA signal. Future research includes obtaining data from more patients and looking into other image feature and metrics to compare PA signal in various tissues.

References

[1] E. Morgan, M. Arnold, A. Gini, V. Lorenzoni, C. Cabasag, M. Laversanne, J. Vignat, J. Ferlay, N. Murphy, and F. Bray, "Global burden of colorectal cancer in 2020 and 2040: incidence and mortality estimates from globocan," *Gut*, vol. 72, no. 2, pp. 338–344, 2023.

[2] CDC-USA, "What are the risk factors for colorectal cancer," 2021.

[3] S. Shinji, T. Yamada, A. Matsuda, H. Sonoda, R. Ohta, T. Iwai, K. Takeda, K. Yonaga, Y. Masuda, and H. Yoshida, "Recent advances in the treatment of colorectal cancer: A review," *Journal of Nippon Medical School*, vol. 89, no. 3, pp. 246–254, 2022.

[4] S. L. Liu and W. Y. Cheung, "Role of surveillance imaging and endoscopy in colorectal cancer follow-up: quality over quantity?" *World journal of gastroenterology*, vol. 25, no. 1, p. 59, 2019.

[5] G. Yang, E. Amidi, W. C. Chapman Jr, S. Nandy, A. Mostafa, H. Abdelal, Z. Alipour, D. Chatterjee, M. Mutch, and Q. Zhu, "Co-registered photoacoustic and ultrasound imaging of human colorectal cancer," *Journal of biomedical optics*, vol. 24, no. 12, pp. 121 913–121 913, 2019.

[6] Y. Zhou, J. Yao, and L. V. Wang, "Tutorial on photoacoustic tomography," *Journal of biomedical optics*, vol. 21, no. 6, pp. 061 007–061 007, 2016.

[7] X. Leng, E. Amidi, S. Kou, H. Cheema, E. Otegbeye, W. J. Chapman, M. Mutch, and Q. Zhu, "Rectal cancer treatment management: deep-learning neural network based on photoacoustic microscopy image outperforms histogram-feature-based classification," *Frontiers in Oncology*, vol. 11, p. 715332, 2021.

[8] N. Sato, M. K. A. Singh, Y. Shigeta, T. Hanaoka, and T. Agano, "High-speed photoacoustic imaging using an led-based photoacoustic imaging system," in *Photons Plus Ultrasound: Imaging and Sensing 2018*, vol. 10494. SPIE, 2018, pp. 268–272.

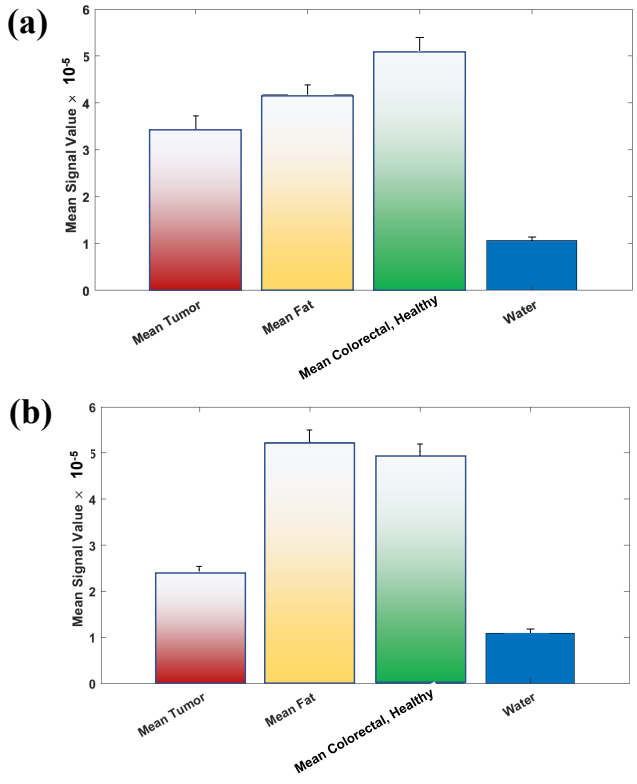

Fig. 3. Pixel-based analysis for two images (a) and (b), which contained all tissues of interest in one frame. The mean of pixel values in selected regions in tumor (1,2), fat (3,4), healthy colon tissue (5,6), and water/noise (7,8) are presented and the standard errors are shown on top of the bars for each region.